

2.D Thermal Self-Focusing with Multiple Laser Beams

Self-focusing in the long-scale-length coronas of reactor targets may enhance undesired parametric processes and may lead to the degradation of drive uniformity. Both the ponderomotive and thermal modes are of potential importance. In this article our concern is primarily with the thermal mode, which is amenable to simulation using the hydrodynamics/ray-tracing code SAGE.^{1,2} Hydrodynamic simulations of thermal self-focusing have the advantage that the time history of the plasma under laser heating, thermal conduction, and two-dimensional hydrodynamic flow can be followed, in contrast to simple perturbation models in which (a) plasma properties vary in one dimension only (transverse to the laser propagation direction); (b) the perturbed temperature and density profiles are related by static pressure balance; and (c) refraction near critical is excluded.

For multibeam laser-irradiation systems such as OMEGA it is of interest to investigate self-focusing effects associated with multiple overlapping laser beams. While this is a fully three-dimensional problem, insight may be gained from two-dimensional simulations. Here we use Cartesian geometry, with variations of plasma parameters and ray trajectories permitted in the (x,y) plane. Cylindrical or spherical geometries could alternatively be used, with the laser beams treated as annular rings. The simulations presented here make use of a recent enhancement to SAGE whereby any number of independent laser beams may be specified, each with its own wavelength, temporal and spatial profiles, angle of incidence, and focusing parameters.

Thermal and Ponderomotive Self-Focusing

Models of self-focusing generally consider a uniform laser beam of wavelength λ and intensity I propagating through a plasma of electron temperature T_e , electron density n_e , and critical density n_c . It is assumed that superimposed upon the beam is an intensity perturbation, or "hot spot," with a wavelength λ_{\perp} transverse to the direction of propagation. In the simplest theory of ponderomotive self-focusing³ (sometimes known as filamentation), whether or not the perturbation will grow depends only on the balance between two physical processes, the ponderomotive force and diffraction. The ponderomotive force pushes plasma away from the higher-intensity portions of the beam, causing the beam in these regions to converge due to the resultant refractive-index change, and thereby enhancing the perturbation. Counteracting this tendency, diffraction always causes the higher-intensity portions to diverge. Whatever the parameters of the laser and the plasma, the theory predicts that there is a threshold wavelength λ_{th} such that no growth is possible for λ_{\perp} less than λ_{th} but growth occurs for any λ_{\perp} greater than λ_{th} . Maximum growth occurs for $\lambda_{\perp} = \lambda_p (= \sqrt{2} \lambda_{th})$:

$$\lambda_p = 3.273 \times 10^2 \left(\frac{T_e}{I} \frac{n_c}{n_e} \right)^{1/2} (1 - n_e/n_c)^{1/4} \text{ cm}, \quad (1)$$

where T_e is in eV and I in W/cm^2 .

It is important to note that all plasmas are unstable to (ponderomotive) self-focusing, for sufficiently large perturbation wavelengths λ_{\perp} . The crucial parameter, however, is the growth length L through which the intensity perturbation is amplified by a factor of e . Significant growth may be expected if the scale length of the coronal plasma exceeds L . For maximum growth ($\lambda_{\perp} = \lambda_p$), the growth length is given by

$$L_p = 3.409 \times 10^4 \frac{T_e}{I\lambda} \left(\frac{n_c}{n_e} - 1 \right) \text{ cm}, \quad (2)$$

where λ is in centimeters. For larger transverse wavelengths ($\lambda_{\perp} > \lambda_p$), the growth length increases slowly ($L/L_p \approx 0.7 \lambda_{\perp}/\lambda_p$ for $\lambda_{\perp} \geq 2\lambda_p$).

A similar picture holds for thermal self-focusing, except that here it is the thermal pressure of heated plasma rather than the ponderomotive force that pushes the plasma laterally. In perturbation treatments⁴ the plasma temperature profile in the lateral direction is determined by balancing laser-energy deposition with thermal diffusion, and the density profile is then obtained assuming lateral pressure balance ($n_e T_e = \text{constant}$). While this treatment neglects time-dependent hydrodynamics, and uses Spitzer's formula⁵ for the lateral heat flux in a regime in which it almost certainly breaks down, it is nevertheless useful as a guide to the parameter regimes in which thermal self-focusing is liable to be found.

For thermal self-focusing there is a transverse wavelength threshold:

$$\lambda_T = 14.5 A_0^{1/2} \left(\frac{n_c}{n_e} \right)^{3/4} \frac{\lambda T_e^{5/4}}{Z^{1/2} I^{1/4}} \text{ cm}, \quad (3)$$

where Z is the ion charge state and A_0 is a number close to unity. For perturbation wavelengths $\lambda_{\perp} < \lambda_T$ no growth occurs because diffraction is dominant. For $\lambda_{\perp} > \lambda_T$, the growth length is almost independent of λ_{\perp} and is given by

$$L_T = 67.0 A_0 \left(\frac{n_c}{n_e} \right)^{3/2} \frac{\lambda T_e^{5/2}}{Z I^{1/2}} \text{ cm}. \quad (4)$$

As an illustration of the use of these formulae, Table 28.II gives the values of L_T , λ_T , L_p , and λ_p for a wavelength $\lambda = 250 \text{ nm}$ (krypton fluoride laser), $I = 10^{15} \text{ W/cm}^2$, and $Z = 3.5$ (CH), for two temperatures (6 keV and 1 keV) and two regions in the corona (quarter and tenth critical). The higher temperature would correspond to the peak of a shaped reactor pulse, and the lower temperature to the early, lower-intensity portion of the pulse. For $T_e = 6 \text{ keV}$, the thermal growth

length L_T is very large, several times greater than the millimeter scale length anticipated for a reactor plasma. L_T may be an overestimate, however, because the assumption of Spitzer conductivity leads to an unreasonably strong temperature dependence [see Eq. (4)]. On the other hand, for $T_e = 1$ keV, L_T becomes much less than a millimeter. It therefore appears that thermal self-focusing is of greatest concern for target designs that result in the generation of a relatively cold long-scale-length plasma early in the pulse.

The ponderomotive mechanism is clearly important for both temperatures. Its effects may possibly be mitigated by using overlapping beams, so that a high average intensity on the surface of a sphere would be obtained from a large number of individual beams each with an intensity below the threshold for significant self-focusing. Alternatively, the use of ISI techniques⁶ may suppress self-focusing.

Table 28.11
Growth lengths and transverse wavelength (microns) for thermal and ponderomotive self-focusing.

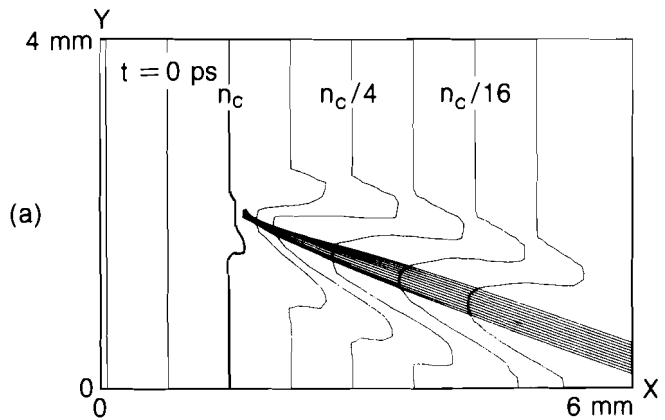
	$T_e = 6$ keV				$T_e = 1$ keV			
	Thermal		Ponderomotive		Thermal		Ponderomotive	
	L_T	λ_T	L_P	λ_P	L_T	λ_T	L_P	λ_P
$n_c/4$:	3,380	51	240	15	40	5	40	6
$n_c/10$:	13,300	102	740	25	150	11	120	10

TC2078

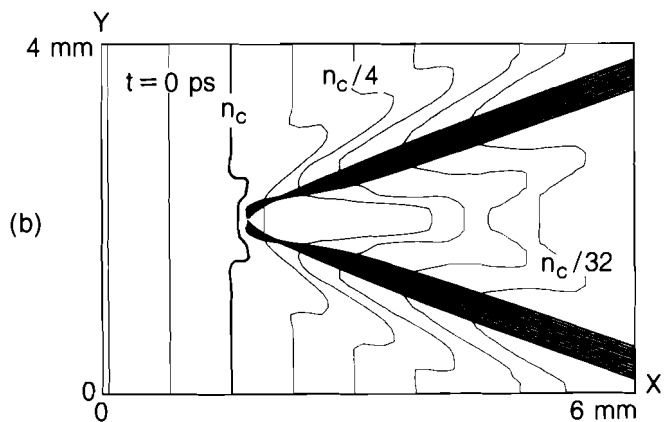
Hydrodynamic Simulations

In a typical simulation [see Fig. 28.15(a)] a hot spot is represented by a 1.5-ns beam (full width at half maximum), with a nominal intensity of 3×10^{15} W/cm² based on the area in the target plane containing 90% of the energy. The beam is incident at an angle of 20° upon a cold preformed plasma with an exponential density profile of scale length 1 mm.

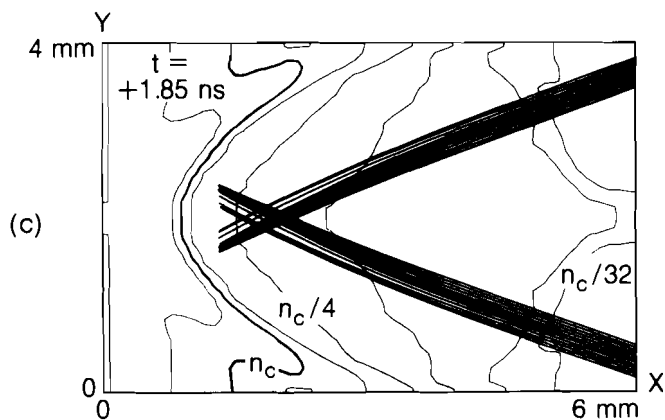
Here, as well as in subsequent simulations, the laser has a wavelength of 351 nm, and Gaussian temporal and spatial profiles. Rays are plotted up to the point at which 90% of their energy has been deposited, although their trajectories are calculated until all but one part in 10^5 is absorbed. Only a subset of the rays actually used is plotted. The marginal rays have intensities that are 10% of the peak intensity; the beam is truncated beyond these bounds in order that the figures provide a useful representation of the spatial location of the beam energy. A flux limiter f equal to 0.04 is used.⁷ (The effect of varying the flux limiter was investigated in Ref. 1). By the peak of the pulse ($t = 0$), a self-focusing channel is apparent in the underdense plasma.



RUN 1903
TC2023



RUN 1904
TC2024

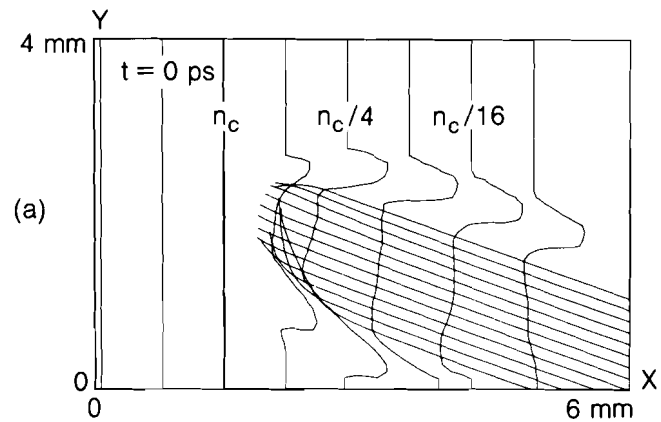


RUN 1904
TC2025

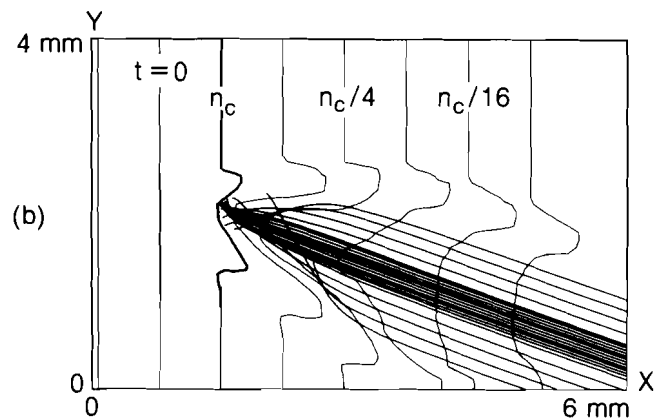
Fig. 28.15
Self-focusing of single and overlapping beams in a long-scale-length preformed plasma. In (a) a single beam is incident in Cartesian geometry at 20° to the target normal, forming a self-focusing channel in the corona. In (b) a second beam, identical except for the angle of incidence, is added. Two independent self-focusing channels are formed. At a later time (c), plasma ablation has removed the channels and the two beams propagate independently through the plasma.

In order to examine the effect of overlapping beams, a second beam, identical except for the angle of incidence, is added in Figs. 28.15(b) and 28.15(c). The two beams are pointed so as to overlap on the initial critical surface. At the peak of the pulse [$t = 0$, Fig. 28.15(b)], two largely independent channels are seen, with a high-density region formed between the two beams. Later in time [$t = +1.85$ ns, Fig. 28.15(c)], the channels have merged, plasma ablation has led to the termination of self-focusing, and the two beams pass through each other. The transient nature of thermal self-focusing is a characteristic feature of these and earlier simulations.¹

A second configuration of interest is that of a hot spot superimposed upon a beam of larger diameter. An example is provided in Fig. 28.16. In Fig. 28.16(a) a single beam of Gaussian spatial profile, diameter 1.2 mm and intensity 1.5×10^{15} W/cm², is seen not to self-focus, aside from a few marginal rays being refracted inward. This is as expected,



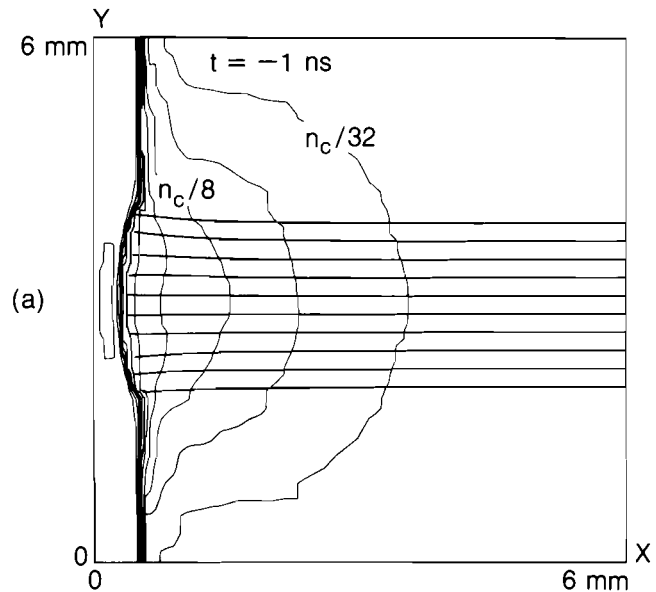
RUN 1905
TC2026



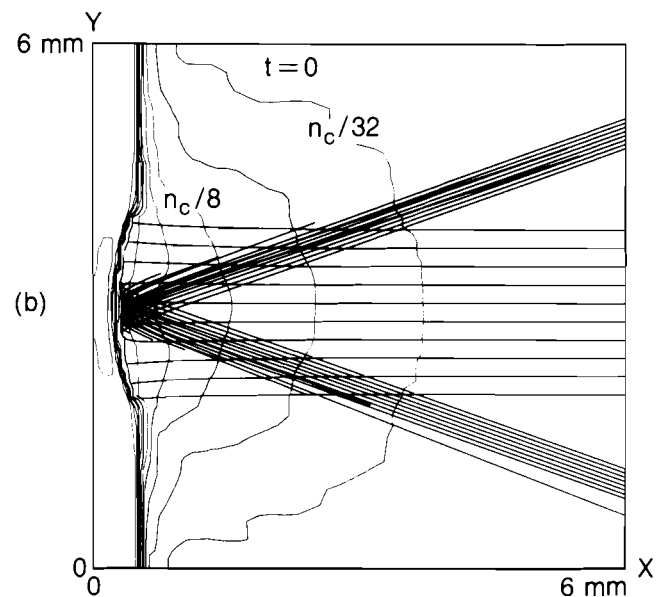
RUN 1906
TC2027

Fig. 28.16
Effect of a hot spot superimposed on a background beam. In (a) a broad background beam propagates through a long-scale-length preformed plasma largely unaffected by refraction. In (b), with 50% of the energy redistributed into a small-diameter hot spot, the hot-spot beam self-focuses and also causes rays from the background beam to be refracted in toward the focus.

because the beam diameter exceeds the plasma scale length.¹ For the simulation shown in Fig. 28.16(b), 50% of the energy of the single beam is redistributed into a hot spot of diameter 0.3 mm, intensity 3×10^{15} W/cm², and the same temporal profile. Here strong self-focusing is initiated in the hot spot, causing rays from the large-diameter beam to be refracted inward toward the focus. Thus a hot spot can degrade illumination uniformity over more than its own area.



RUN 1907
TC2028



RUN 1907
TC2029

Fig. 28.17
Suppression of thermal self-focusing in a heated background plasma. Two small-diameter short-pulse beams, representing hot spots, are incident (obliquely) on a plasma produced by a large-diameter long-pulse beam of lower intensity, which might represent the early portion of a shaped reactor pulse. The coronal plasma produced by the long-pulse beam 1 ns before the onset of the short-pulse beams (a) is hardly perturbed by the time of the peak of the short-pulse beams (b).

It may be argued that these simulations are not applicable to reactor conditions, on account of the assumption of a cold preformed plasma. It is probably more realistic to consider a configuration in which the plasma is formed by a large-diameter long-pulse beam, with a small-diameter short-pulse hot spot incident upon the plasma after some time delay. Results from such a simulation are shown in Fig. 28.17, where two overlapping hot spots are used to interact with the long-scale-length plasma. Here a 10-ns beam of diameter 1.6 mm and intensity 6×10^{14} W/cm² forms a CH plasma of scale length ~ 1 mm below quarter-critical and with a coronal temperature ~ 3 keV, just before the onset of the hot spots [Fig. 28.17(a)]. The additional beams, of intensity 4×10^{15} W/cm², duration 1 ns, and diameter 0.3 mm, represent large-amplitude intensity perturbations and are synchronized to the peak of the 10-ns beam. The plasma appears to be perturbed very little by these hot spots [Fig. 28.17(a)], confirming the expectation that thermal self-focusing is less important for hot plasmas. This result is independent of whether the hot spots are incident normally or obliquely.

Summary

In the presence of overlapping laser beams, transient self-focusing effects occur in which the density perturbation of one beam affects the ray trajectories of another. Thermal self-focusing is probably not important for hot reactor plasmas, at least for the low-Z materials we have modeled, but the process may well be of concern for any target designs that result in the generation of a relatively cold long-scale-length plasma early in the laser pulse.

ACKNOWLEDGMENT

This work was supported by the U.S. Department of Energy Office of Inertial Fusion under agreement No. DE-FC08-85DP40200 and by the Laser Fusion Feasibility Project at the Laboratory for Laser Energetics, which has the following sponsors: Empire State Electric Energy Research Corporation, General Electric Company, New York State Energy Research and Development Authority, Ontario Hydro, Southern California Edison Company, and the University of Rochester. Such support does not imply endorsement of the content by any of the above parties.

REFERENCES

1. R. S. Craxton and R. L. McCrory, *J. Appl. Phys.* **56**, 108 (1984). See also LLE Review **18**, 72 (1984).
2. R. S. Craxton and R. L. McCrory, Laboratory for Laser Energetics Reports 99 and 108 (1980).
3. B. I. Cohen and C. E. Max, *Phys. Fluids* **22**, 1115 (1979).
4. M. J. Herbst *et al.*, NRL Memorandum Report 4983 (1982).
5. L. Spitzer and R. Härm, *Phys. Rev.* **89**, 977 (1953).
6. S. P. Obenschain *et al.*, *Phys. Rev. Lett.* **56**, 2807 (1986).
7. R. C. Malone, R. L. McCrory, and R. L. Morse, *Phys. Rev. Lett.* **34**, 721 (1975).